Int. J. Electrochem. Sci., 10 **(2015)** 1054 - 1064

International Journal of
ELECTROCHEMICAL
SCIENCE
www.electrochemsci.org

Multifractal Hurst Analysis for Identification of Corrosion Type in AISI 304 Stainless Steel

William Sanchez-Ortiz[1], *Coral Andrade-Gómez*[2], *Eliseo Hernandez-Martinez*[2] *and Hector Puebla*[1,*]

[1]División de Ciencias Básicas e Ingeniería. Universidad Autónoma Metropolitana, Av. San Pablo #180 Col. Reynosa Tamaulipas, Del. Azcapotzalco, México, D.F., CP 02200, MÉXICO
[2] Facultad de Ciencias Químicas, Universidad Veracruzana-Región Xalapa, Calle de la Pergola S/N, Zona Universitaria, Xalapa Ver., CP 91090, MEXICO
[*]E-mail: hpuebla@correo.azc.uam.mx

Received: 16 October 2014 / *Accepted:* 17 November 2014 / *Published:* 16 December 2014

Fractal analysis methods are able to characterize complex time-series and images. In electrochemical corrosion, fractal parameters (fractal dimension, scaling exponent, correlation factors, etc.) have been correlated to the corrosion mechanism, the surface roughness and long-term behavior. In this work, a two-dimensional re-scaled Hurst analysis method has been utilized for determining the scaling Hurst exponent resulting from the electrochemical corrosion of AISI 304 stainless steel (SS) exposed to $FeCl_3$ and NaOH solutions. It is found that the AISI 304 SS exposed to $FeCl_3$ a NaCl solutions exhibits positive correlations and multifractal properties. In order to quantify the complexity of the corroded surfaces and establish a correlation with the corrosion type a multifractal index is calculated.

Keywords: Multifractal analysis, corrosion type, 304 stainless steel.

1. INTRODUCTION

AISI 304 stainless steel (SS) is a commercial grade of austenitic SS that is widely used in many conventional applications due its ability to form protective oxide film on its surface for corrosion resistance in oxidizing environments. [1]. However, the exposure of SS to different corrosive solutions leads to localized corrosion such as pitting or intergranular corrosion. Therefore, it is necessary to know the conditions that the corrosion is produced and at the same time the prevention methodologies.

For the corrosion characterization of AISI 304 SS in different corrosion environments ~~several~~ different conventional methods have been applied. For instance, electrochemical noise (EN) measurements, electrochemical impedance spectroscopy (EIS) and DC polarization measurements [2-

7]. Image analysis of high-resolution micrographs of corroded surfaces by visual and statistical methods has been also used to this end [8-12].

Non-conventional analysis for corrosion characterization includes fractal analysis from both time series obtained from the EN technique and images of corroded surfaces. Fractal analysis of time series and images is characterized for the determination of correlations between macroscopic physical properties and fractal parameters [13-16]. For instance, EN data of corrosion systems has been studied by several authors via different fractal methods [17-20]. Planinsic and Petek [17] proposed the corrosion characterization by means of the estimation of fractal dimension in EN signals. Their results showed that fractal dimension can be used as an index for the classification of the corrosion-type. Using the rescaled range Hurts analysis Lopez et al. [18] and Amaya et al. [19] reported multifractality in time series of the potential electrochemical noise of copper in sea water and of API X52 pipeline steel in a media containing sulphate reducting bacteria. Fractal analysis ~~have~~ has also been realized for the quantification of the performance of corrosion inhibitors. For example, Sarmiento et al. [20] used the rescaled range Hurts analysis in EN time series, finding that the Hurst exponent index helps to evaluate the inhibitor protection in corrosion. These results were validated by EIS. Liu et al. [21] introduce a fractal parameter computed using the wavelet transform which extract the local feature of electrochemical noise and quantitatively describe the change of its fractal characteristic with time.

Fractal analysis has been also applied to micrograph images to characterize the surface roughness of corroded materials [22-25]. For instance, Wang et al. [24] used a two-dimensional wavelet analysis for corrosion identification via the computed fractal dimension. Garcia-Ochoa and Corvo [25] study the copper patina corrosion by means of fractal geometry using EN and image analysis. They found a direct relationship between fractal analysis of EN time series and images.

In this work the application of multifractal analysis <u>to</u> of optical micrograph images taken from AISI 304 SS plates exposed to two corrosive media (i.e., aqueous solutions of $FeCl_3$ and NaOH) was explored. Single fractal analysis leads to a statistical measure of the whole object, i.e. it represents a measure of its global complexity and, hence, demonstrates the fractal properties of the object as a whole. On the other hand, multifractal analysis explores fractal properties of different local regions ~~loci~~ within the object. Multifractal analysis can reveal that objects have global and different local fractal dimensions and, hence, local differences in complexity. To the best of the author´s knowledge, despite that multifractality features in the literature have been reported in EN data of different corrosion systems, multifractal analysis from images of corroded surfaces has not been explored. An attempt to correlate the corrosion type was also made via a multifractality index. The results showed multifractal features of the studied corrosion systems and suggest that the proposed multifractality index can be used to distinguish the corrosion type.

This paper is organized as follows. In Section 2 materials and methods are described. Results are presented and disused in Section 3. Finally, concluding remarks are provided in Section 4.

2. MATERIALS AND METHODS

In this section materials and methods for the image analysis are described. The two dimensional fractal analysis method for image fractal characterization is also presented.

2.1 Image analysis

Analytical grades (Merck) of NaOH and $FeCl_3$ and deionized water were used for preparing the test solution, 0.1 and 0.5 M, respectively. The sample was pretreated by mechanical polishing with abrasive grade paper. Two identical AISI 304 SS plates were constructed and exposed to the aqueous solution of NaOH and $FeCl_3$ during eight hours.

Optical microscopy was carried out with the aid of an OLYMPUS PMG3 microscope that served to examine the surface morphology of the exposed samples. The samples with an exposure time of eight hours were metallographically polished and the cross section was analyzed to investigate the morphology of the corroded surface. Optical micrographs were taken at various magnifications (5, 10, 20 and 50μm).

2.2 Fractal analysis

The rescaled range (R/S) Hurst analysis has been applied to the estimation of the fractal characteristics of time-series and images. In particular, R/S two dimensional analysis has been for the characterization of image of a wide variety of applications. The description of the R/S two dimensional method is as follows:

1. Transform the image to gray scale, where is assign a numerical value to each pixel (i.e., 0 to 256) leading to a *N* x *M* matrix, where *N* and *M* are the number of pixels from the original image in the vertical and horizontal directions, respectively.

2. For a matrix $X_{N,M} = (x_{i,j})$ is considered a subsample of N_k x M_k-dimensional, $Y_{N_k,M_k} = (y_{i,j})$ where $N_k = sN$ and $M_k = sM$ (the matrix subsample keeps the row-columns relation) and s determinates the subsample size.

3. Compute the average of the subsample N_k as,

$$\bar{y}_S = \frac{1}{N_k M_k} \sum_{i=1}^{N_k} \sum_{j=1}^{M_k} y_{i,j} \quad (1)$$

4. A partial sum sequence is calculated as,

$$z_i = \sum_{i=1}^{N_k} \sum_{j=1}^{M_k} (y_{i,j} - \bar{y}_s) \quad (2)$$

5. The re-escalated range is determined with $(R/S)_S = R_S / \sigma_S$, where $R_S = \max\{z_i\} - \min\{z_i\}$ is the range of partial sums and σ_S is the subsample's standard deviation, which is given by

$$\sigma_S = \left[\frac{1}{N_k M_k} \sum_{i=1}^{N_k} \sum_{j=1}^{M_k} (y_{i,j} - y_S)^2 \right]^{\frac{1}{2}} \quad (3)$$

The above steps can be summarized as,

$$(R/S)_S = \frac{1}{\sigma_S}\left[\max_{\substack{1\le i\le N_k\\ 1\le j\le M_k}}\sum_{l=1}^{i}\sum_{n=1}^{j}(y_{l,n}-\bar{y}_S) - \min_{\substack{1\le i\le N_k\\ 1\le j\le M_k}}\sum_{l=1}^{i}\sum_{n=1}^{j}(y_{l,n}-\bar{y}_S)\right] \quad (4)$$

R/S analysis indicates that the re-scaled range must be calculated in a sufficiently large number of submatrix Y_{N_k,M_k} of different sizes s. If the stochastic process associated with the sequence $X_{N,M}$ is scaled on a certain domain $s \in (s_{\min}, s_{\max})$, the statistic R/S follows a power law, such as

$$(R/S)_S = as^{2H} \quad (5)$$

where a is a constant and H is the scaling Hurst exponent, which is a measurement of the fractal sequence correlations. A log-log graph $(R/S)_S$ as a function of the scale squared, $s \in (s_{\min}, s_{\max})$ generates a line with slope H. It has been concluded in [26] that the relationships among the Hurst exponent and correlations of an image sequence are as following: (i) If H=0.5 indicates no correlations. (ii) If H > 0.5 indicates the persistent of the image surface, i.e. the surface has a strong tendency to return to the neighboring values, and differences between adjacent points are small. (iii) If H < 0.5 indicates anti-persistent of the image surface, i.e. the surface has a tendency to diverge of the neighboring values leading to significant differences between adjacent points are significant [26]. Thus, the interpretation of the parameter H can also related to the roughness of the image surface: the closer H to 0, the rougher image and the closer H to 1, the smoother the corresponding texture.

2.3 Multifractal analysis

Multifractality is a useful tool for explaining many patterns seen in nature. In particularly, multifractal analysis allows to investigate a mixture of fractal dimensions characterize the inherent complexity in some data series. Based on the thoughts of Barabasi and Vicsek [27], and Katsuragi and Honjo [28], the multifractal analysis can be done through the calculation of the rescaled range by means of the q-moment of σ_s, that is,

$$\sigma_{S,q} = \left[\frac{1}{N_k M_k}\sum_{i=1}^{N_k}\sum_{j=1}^{M_k}(y_{i,j}-y_S)^q\right]^{\frac{1}{q}} \quad (6)$$

In this case, the range is given by $(R/S)_{s,q}=R_s/\sigma_{s,q}$, and the average range is expected to follow the scaling behavior $(R/S)_{S,q} = as^{2H_q}$, where H_q is the q-th Hurst exponent. If H_q is constant for all q then the underlying image is monofractal. A non-trivial dependence of H_q on q indicates that the process is multifractal. It should be recalled that a multifractal system is a generalization of a fractal system in which a single exponent (the fractal dimension) is not enough to describe its dynamics. In general, multifractality also indicates the nonlinear nature of the mechanisms that generated the series. To describe the degree of multifractality in the images, we propose a multifractality index defined as,

$$I_M = \max(H(q)) - \min(H(q)) \quad (7)$$

where $H(q)$ is the H value as a function of q.

3. RESULTS AND DISCUSSION

In this section the results of the optical microscopy and of the fractal and multifractal analysis are presented and discussed.

3.1 Optical microscopy

Figures 1 and 2 shown the optical micrographs at different magnifications (i.e., 5, 10, 20 and 50μm) of AISI 304 SS plates exposed eight hours in aqueous solutions of $FeCl_3$ and NaOH, respectively. As expected, it can be observed, by visual inspection, from Figure 1 that the nature of attack on the surface of the plate exposed to $FeCl_3$ leads to pitting corrosion. While the plate exposed to NaOH presents uniform corrosion, which affect all surface. Thus, a major roughness is displayed for the plate exposed to NaOH 0.1 M aqueous solution than the plate exposed to the $FeCl_3$ 0.5 M solution.

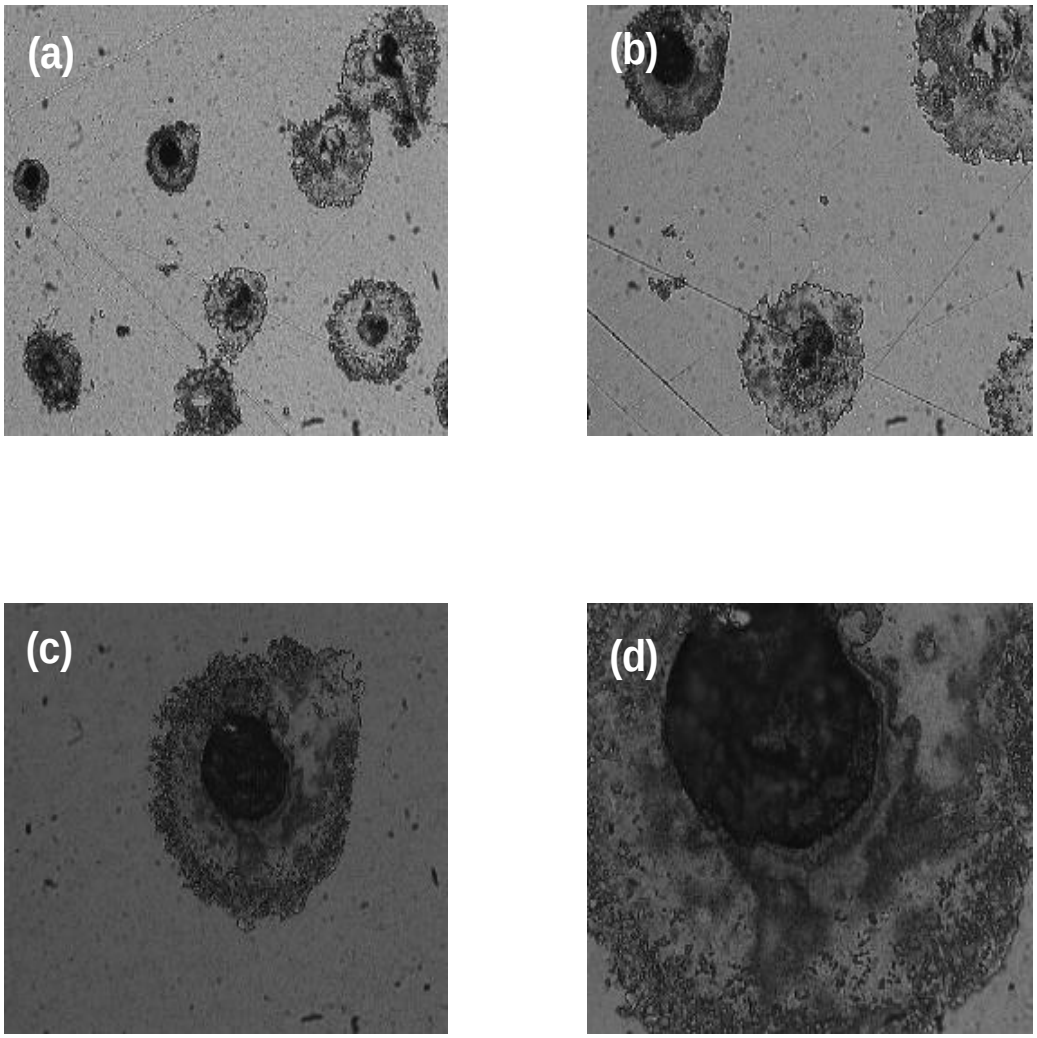

Figure 1. Optical micrograph of the SS exposed to FeCl.

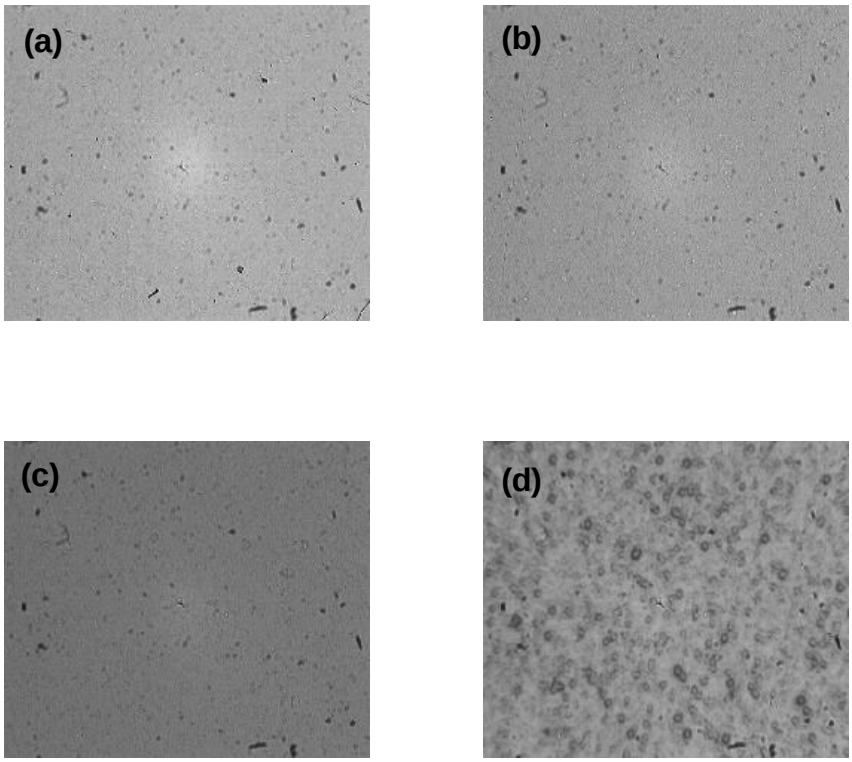

Figure 2. Optical micrograph of the SS exposed to NaOH.

3.2 Fractal analysis

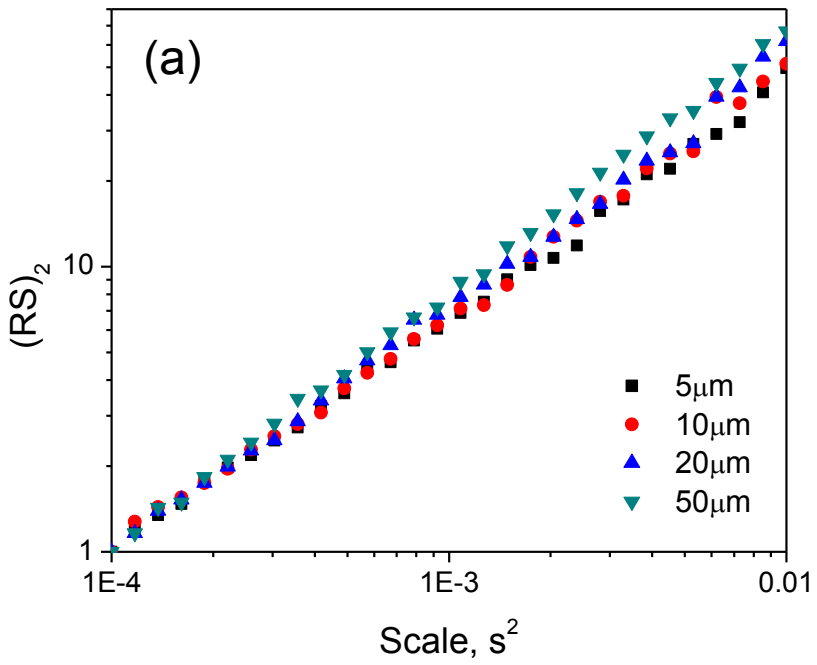

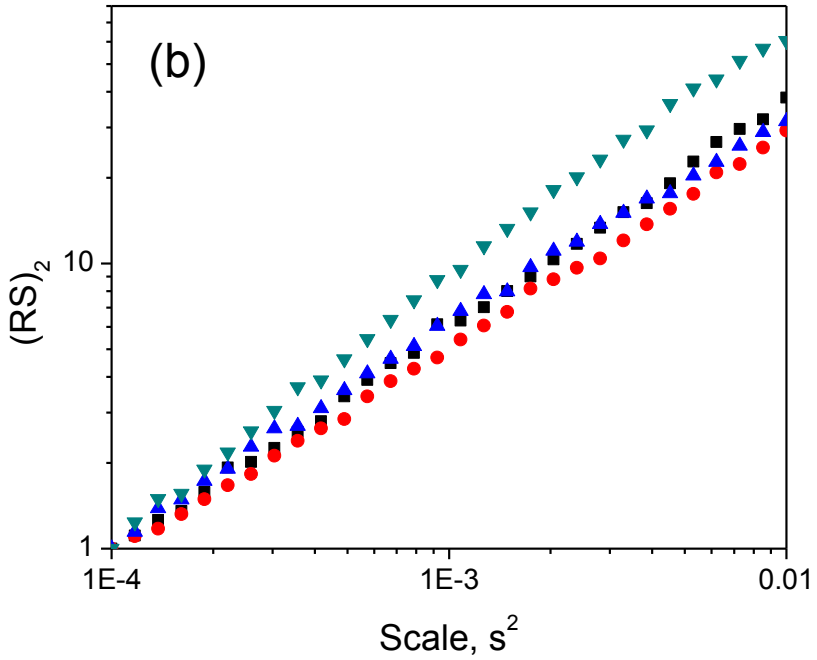

Figure 3. Hurst exponent $H_2(s)$ as a function of scale s to different magnifications, a) FeCl and b) NaOH solutions.

Figure 3 shows the results obtained with the single fractal R/S analysis, i.e. for the q-norm equal to 2. The Hurst exponent values and the fractal dimension (computed via the relationship $D = 3 - H(2)$), for different magnifications of the optical micrographs, are $H(2) = 0.85 \pm 0.04$ and $D = 2.15 \pm 0.04$ and $H(2) = 0.79 \pm 0.045$ and $D = 2.21 \pm 0.045$, for $FeCl_3$ and NaOH solutions, respectively. Hurst exponent result suggests the presence of fractal properties of the corroded surfaces and persistent behaviors of the corresponding corrosion mechanisms.

The fractal geometry on the corroded surfaces is apparent via the self-similarity of the optical micrographs. For the case of the plate exposed to NaOH 0.1 M solution, optical micrographs at different magnifications revels an apparent uniform distribution of small pits along the corroded surface. On the other hand, the optical micrograph of corroded surface exposed to $FeCl_3$ 0.5 M solution shows large and small pits at the different levels of magnification.

The persistent behavior is presumably related to the corrosion mechanism generating the corroded surfaces. In the case of pitting corrosion, the persistent behavior can be associated to the birth and continuous growth of corrosion sites in localized areas on the surface. On the other hand, persistence in uniform corrosion can be attributed to the continuous loss of material occurring on the entire exposed surface.

Based on the fractal parameters, i.e. Hurst exponent and fractal dimension, it can be concluded that the corroded surface exposed to NaOH 0.1 M solution displays more roughness than the surface exposed to $FeCl_3$ 0.5 M solution. Indeed, large values of $H(2)$ are associated with more ordered surfaces and large departures from the fractal dimension 2 indicates more fractality. The more roughness of the corroded surface exposed to NaOH 0.1 M solution is attributed to the uniform

irregularity on the whole surface compared with a combination of localized irregularities and smooth regions of the surface exposed to $FeCl_3$ 0.5 M solution.

In general, our results are consistent with similar fractal studies reported in the literature using EN data and images of corroded surfaces in different media [18-20]. Indeed, persistence behavior of corrosion mechanism has been reported in several studies. On the other hand, it is noted that despite there is not a unique fractal dimension measure, our results are in accordance with other studies reporting the fractal dimension using other methods, i.e. more roughness for passive and uniform corrosion that localized or pitting corrosion [24].

3.3 Multifractal analysis

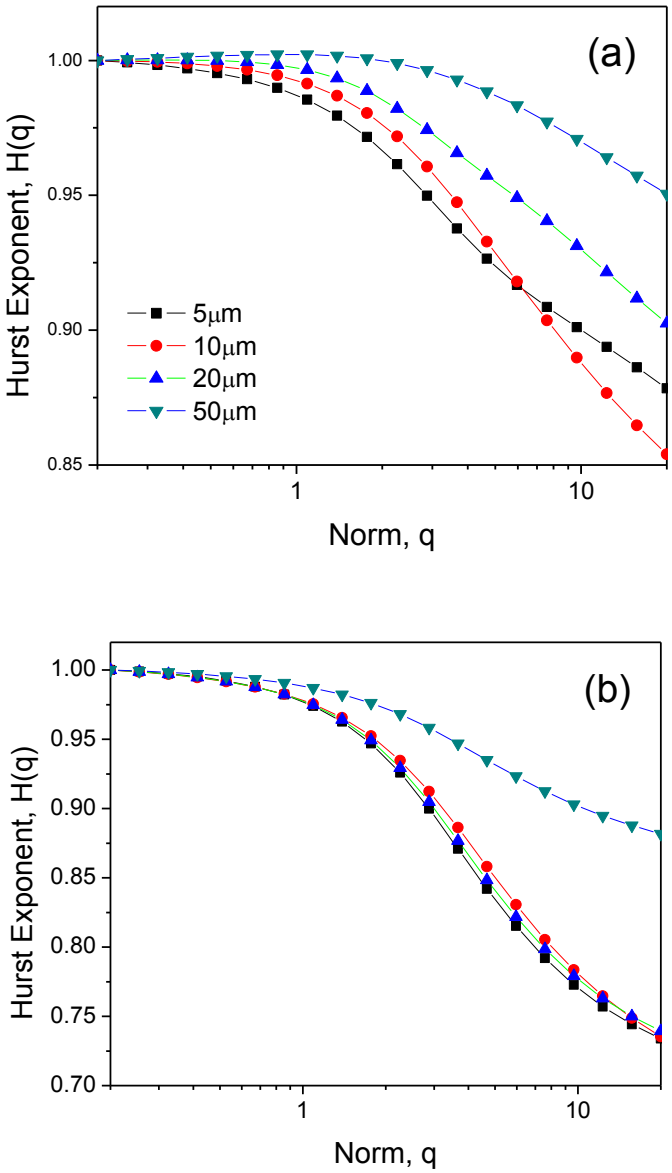

Figure 4. Variations of Hurst exponent with *q* parameter, showing the existence of multifractality in SS corrosion images, a) FeCl and b) NaOH solutions.

Figure 4 shows the variation of normalized *H* values as a function of *q*-norm. It can be observed from this figure nonlinear variation of Hurst exponent as a function of the *q*-norm, indicating the presence of multifractal properties on AISI 304 SS corroded surfaces for both corrosion media. From Figure 4, it also can be observed that Hurst exponents increases with the increase of magnification. Thus, for the same corrosion system and different magnifications, the fractal dimension decreases for higher magnifications.

Multifractality of electrochemical noise corrosion data has been reported by some authors [18,19]. They have pointed out that mutifractality in corrosion systems is a consequence of several local differences of complexity. Indeed, corrosion is a very complex phenomena, that includes birth and growth of corrosion sites, passivation, breaking of passive layer, repassivation, etc.

Several authors have been stated that differences in fractal properties for different corrosion mechanisms can be used to distinguish the corrosion type of materials [10, 11, 20, 24]. To this end, MI described in above section is computed. Figure 5 shows the MI computed at different magnifications of the optical micrographs. It is interesting to note that for AISI 304 SS plate exposed to $FeCl_3$ the MI value is affected by the scale micrograph. As the scale magnification decrease the MI increases, which can be related to a major complexity in the structure of the surface.

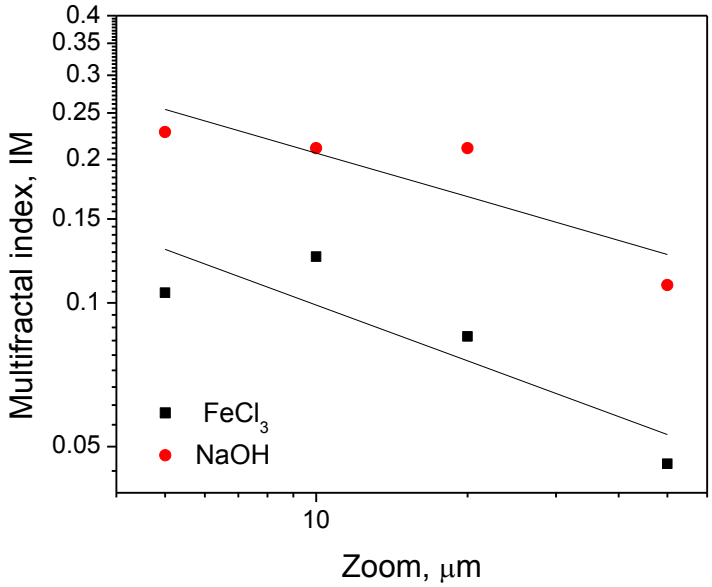

Figure 5. Multifractal index to different magnifications, a) FeCl and b) NaOH solutions.

It also can be observed from Figure 5 that the variation of MI is described by a power law with a negative slope of 0.388. Similar correlations are identified in AISI 304 SS plate exposed to NaOH where the slope is 0.308, indicating major complexity at different scales of damage surfaces by pitting corrosion.

It is also noted that the MI values calculated for NaOH solution are greater than these obtained for FeCl3, suggesting that the structure surface in a passive corrosion is more complex than one

generated in pitting corrosion. Then, MI might be used as a parameter to determine the type of corrosion of AISI 304 SS in different corrosive environments.

4. CONCLUSIONS

This paper presents the use of multifractal Hurst analysis for the characterization of optical micrographs from AISI 304 SS plates exposed to corrosive solutions of $FeCl_3$ and NaOH. Our results indicate that the Hurst exponent provide information about corrosion-type independent from the image magnification. Furthermore, it was observed that the Hurst exponent exhibits a nonlinear variation with q-norm of the standard deviation, which indicates the presence of multifractality features of the electrochemical corrosion of AISI 304 SS exposed to aqueous solutions of $FeCl_3$ and NaOH. A multifractal index is proposed to characterize the complexity degree of the underlying corrosion mechanisms. Both the Hurst exponent and the multifractality index can be correlated with the corroded surface, indicating that uniform corrosion exhibits a higher degree of complexity than pitting corrosion. The results suggest that the multifractality index can be used for corrosion-type identification.

References

1. J. Disegi, L. Eschbach, *Injury* 31 (2000), 2-6.
2. S. Torchio, *Corr. Sci.* 20 (1980), 555-561.
3. A.M. Simoes, M.G.S. Ferreira, B. Rondot, M. da Cunha Belo, *J. Electrochem. Society*, 137 (1990), 82-87.
4. M. Drogowska, H. ME, L. Brossard, *J. Appl. Electrochem*. 27 (1997), 169-177.
5. A. Pardo, M. Merino, A.E. Coy, F. Viejo, R. Arrabal, E. Matykina, *Corr. Sci.* 50 (2008), 780-794.
6. S. Girija, U.K. Mudali, H.S. Khatak, B. Raj, *Corr. Sci.* 49 (2007), 4051-4068.
7. L. Freire, M.J. Carmezim, M.G.S. Ferreira, M.F. Montemor, *Electrochim. Acta,* 56 (2011), 5280-5289.
8. J.J. Santana Rodriguez, F.J. Santana Hernández, J.E. González González, *Corr. Sci.* 48 (2006), 1265-1278.
9. A. Dheilly, I. Linossier, A. Darchen, D. Hadjiev, C. Corbel, V. Alonso, *Appl. Microbiol. Biotech.* 79 (2008), 157-164.
10. R.M. Pidaparti, B.S. Aghazadeh, A. Whitfield, A.S. Rao, *Corros. Sci.* 52 (2010), 3661-3666.
11. K.Y. Choi, S.S. Kim, Corrosion Science, *Corr. Sci.* 47 (2005), 1-15.
12. E.N. Codaro, R.Z. Nakazato, A.L. Horovistiz, L.M.F. Ribeiro, R.B. Ribeiro, L.D.O. Hein, *Materials Sci. and Eng. A* 334 (2002), 298-306.
13. H. Berthiaux, V. Mosorov, L. Tomczak, C. Gatumel, J.F. Demeyre, *Chem. Eng. Process.* 45 (2006), 397-403.
14. M. Ren-Niu, Q. Feng-Liang, G. Suo-Yu, F. Chen-Wang, Z. Hong-Yu, *Chem. Eng. Process*. 47 (2008), 642–648.
15. O. Velázquez-Camilo, E. Bolaños-Reynoso, E. Rodriguez, J. Alvarez-Ramirez, *J. Food Eng.* 100 (2010), 77-84.
16. H.O. Mendez-Acosta, E. Hernandez-Martinez, J.A. Jauregui, J Alvarez-Ramirez, H. Puebla, *Biotechnol. and Bioeng.* 30, (2013) 1-9.
17. P. Planinsic, A. Petek, *Electrochim. Acta* 53 (2008) 5206-5214.

18. J.L. López, L. Veleva, D.A. López-Sauri, *Int. J. Electrochem. Sci*, 9 (2014), 1637-1649.
19. M. Amaya, E. Sosa, J.M. Romero, J. Alvarez-Ramirez, M. Meraz, H. Puebla, *Fractals* 12 (2004), 347-354.
20. E. Sarmiento, J.G. González-Rodriguez, J. Uruchurtu, *Surf. Coat. Tech.* 203 (2008), 46–51.
21. X.F. Liu, H.G. Wang, H.C. Gu, *Corr. Sci.* 48 (2006) 1337-1367.
22. A. Mannelqvist, M. Groth, *Appl. Physics A* 73 (2001) 347-355.
23. S. Duttaa, A. Dasb, K. Baratb, H. Roy, *Measurement* 45 (2012) 1140–1150.
24. S.Q. Wang, D.K. Zhang, D.G. Wang, K. Chen, L.M. Xu, S.R. Ge, *Int. J. Electrochem. Sci*, 8, (2013), 2932-2944.
25. E. García-Ochoa, F. Corvo, *Electrochem. Comm.* 12, (2010), 826-830.
26. J. Alvarez-Ramirez, J. Echeverria, E. Rodriguez, *Physica A* 387 (2008), 6452-6462.
27. A.L. Barabasi, T. Vicsek, *Phys. Rev. E* 44 (1991), 2730-2733.
28. H. Katsuragi, H. Honjo, *Phys Rev E* 59 (1999) 254-262.